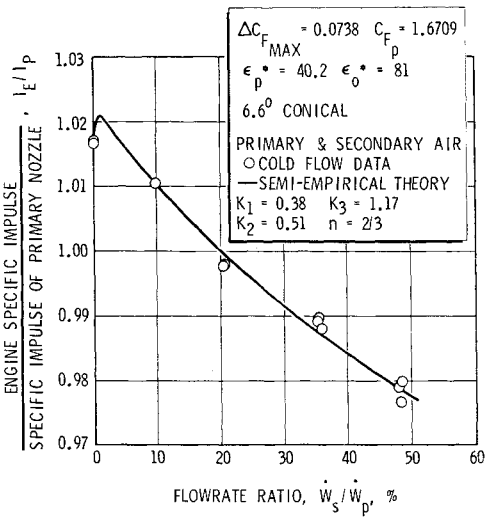

Fig. 7 Aerobell nozzle vacuum specific impulse ratio.

The actual thrust recovery in the extension can be expressed as $\Delta C_F = K_1 \Delta C_{F_{max}}$, where K_1 is a function of nozzle geometry. Experimental data indicate that K_1 is relatively independent of γ_p; therefore, limited testing for each configuration provides adequate empirical information for a wide range of application.

From experimental data and theoretical considerations[1,2] it has been observed that ΔC_F vs ξ behaves as shown in Fig. 3. In Region 1, a rapid increase of ΔC_F results from an interaction between the primary and secondary gases. In Region 2, the effect of secondary flow predominates, and ΔC_F increases linearly with ξ. It is postulated that in Region 2 the secondary flow attains sonic conditions, so that $\Delta C_{F(\text{Region 2})} = K_3 C_{F_s}{}^* \xi + C$, where C accounts for the fact that extension thrust exists even in the absence of secondary flow. C can be expressed[1] in the form $C = K_2 \Delta C_{F_{max}}$, where K_2 is evaluated from experimental data. Experimental data have indicated that K_2 and K_3 are dependent on nozzle geometry but independent of primary and secondary gas properties, and that K_3 is near unity. Thus,

$$\Delta C_{F(\text{Region 2})} = K_2 \Delta C_{F_{max}} + K_3 C_{F_s}{}^* \xi \qquad (13)$$

Experimental data also have indicated that $\Delta C_{F(\text{Region 1})} = K_1 \Delta C_{F_{max}} + B\xi^n$. If the additional restrictions are imposed that ΔC_F and $d(\Delta C_F)/d\xi$ must be continuous at the interface between Regions 1 and 2, the following expressions result

$$B = [(K_2 - K_1)\Delta C_{F_{max}}/(1 - n)]^{(1-n)} [K_3 C_{F_s}{}^*/n]^n \qquad (14)$$

and

$$\xi_0 = [Bn/K_3 C_{F_s}{}^*]^{1/(1-n)} = \xi \text{ at Region 1–2 interface} \qquad (15)$$

For all of the aerobells tested, $n = \frac{2}{3}$. This Region 1 method is simpler than the previously reported method.[2]

Engine vacuum specific impulse is then calculated from

$$I_E/I_p = (1 + \Delta C_F/C_{F_p})/(1 + \dot{w}_s/\dot{w}_p) \qquad (16)$$

Here, I_p is the specific impulse for the basic nozzle up to the step discontinuity.

In conclusion, cold-flow test data or detailed theoretical calculations[1] may be used to obtain the ΔC_F vs ξ plot, Fig. 3, from which constants K_1 through K_3 can be determined as follows: 1) $K_1 = \Delta C_{F(\dot{w}_s = 0)}/\Delta C_{F_{max}}$; 2) $K_2 = \Delta C_{F(2)}/\Delta C_{F_{max}}$ where $\Delta C_{F(2)}$ is the ordinate value obtained by extrapolating the Region 2 curve to $\dot{w}_s = 0$; 3) $K_3 = [d(\Delta C_F)/d\xi]/C_{F_s}{}^*$, where $d(\Delta C_F)/d\xi$ is the Region 2 slope.

Comparison of Theory and Experiment

Nozzles with continuous wall contours

The results of a typical calculation for nozzle performance with secondary injection through slots in the nozzle walls are shown in Tables 1 and 2 and Fig. 4. The value chosen for $P_{os}{}^*$ was determined from Fig. 5, which was constructed using the methods discussed earlier. Note that for the particular point calculation shown, $\dot{w}_s/\dot{w}_p = 1\%$, so that $P_{os}{}^*$ is approximately equal to the secondary manifold stagnation pressure. This is not true for higher flowrate conditions, however, as indicated in Fig. 5.

The analytical results for performance are compared with experimental values in Fig. 4. On the highly enlarged scale, the theory is within the spread of the experimental data (0.2%). Note in Table 2 that the simplified theory, Eq. (11), gives a value of I_E/I_p essentially the same as the "unsimplified" method, Eq. (7). The simplified theory should only be used for $P_{os}{}^*/P_{we} \leq 10$; however, for higher values it yields conservative results.

Aerobell rocket nozzle

The empirical constants evaluated from the cold-flow test data for the nozzle shown in Fig. 1c are listed in Fig. 6. The constants given in Fig. 6 were used to compute ΔC_F vs ξ. The results are plotted as the solid lines. The symbols are averaged experimental data points. The main point to be noted here is that the same set of constants correlated both the air/air and the CF_4/air data for the 6.6° conical aerobell, thus indicating that the empirical scaling method is valid for extrapolating the results to cases with different fluids. Overall performance curves for the configurations tested vs ξ, including the cylindrical aerobells, were previously presented.[2]

A higher area-ratio 6.6° conical aerobell (Fig. 1c) was also tested for $\dot{w}_s/\dot{w}_p$ up to 0.50; the empirical curve for this configuration and the experimental data are shown in Fig. 7.

References

[1] Hosack, G. A. and Stromsta, R. R., "Performance of the Aerobell Extendible Nozzle Rocket Engine," *Journal of Spacecraft and Rockets*, Vol. 6, No. 12, Dec. 1969, pp. 1416–1423.

[2] Stromsta, R. R. and Hosack, G. A., "Analytical Methods for Computing the Effects of Turbine Exhaust and Film Coolant Injection on Rocket Engine Performance," AIAA Paper 69-473, U. S. Air Force Academy, Colo., 1969.

Range Safety Information Analysis

J. T. KOPECEK,* P. STANEK,† AND J. COLLINS‡
Lear Siegler, Inc., Los Angeles, Calif.

SIGNIFICANT improvements in range safety systems could be realized by the use of computer-driven displays that present in real time key elements of the missile flight situation. This would enable the Range Safety Officer (RSO) to maintain a more accurate assessment of actual mission status than is now possible. Less pessimistic destruct criteria could also be used, corresponding to the extent to which uncertainty with respect to actual missile status can be reduced.

Presented as Paper 70-247 at the AIAA Launch Operations Meeting, Cocoa Beach, Fla., February 2–4, 1970; submitted February 27, 1970; revision received July 2, 1970.

* Comanager, Systems Technology Center.
† Senior Scientist, Systems Technology Center.
‡ Consultant. Member AIAA.

The general attributes of range safety systems are fairly well standardized. The missile is monitored by independent tracking, usually a radar system. On-board instrumentation measures rates, chamber pressures, and other critical functions of the vehicle. A third source of information is from the on-board guidance system, although this information is not independent of missile commands, and thus when the missile goes awry, the information from the guidance system could also go awry. Communication with the missile is maintained both passively and actively by telemetry and radar. The flight of the missile is stopped by means of radio communication with the vehicle which either directs cutoff of the fuel to the engines or initiates a destruct charge. With these means available, what should be monitored in order best to establish whether flight should end? One approach is an enhanced range safety system known as EROICA (Enhanced Real Time Operational Impact and Casualty Analyzer). This system offers all the failure-monitoring functions available in current systems and gives a more realistic picture of the impact points and hazards, presenting all the information on a single cathode ray tube (CRT). Its design is based on five steps:

1) The system must sense whether the missile is failing and, if the missile is failing, it must establish where at that time the missile will impact.

2) Since flight termination will result in debris, there will not be a single impact point, but the system should estimate the footprint of all the impact points of all the debris from destruct.

3) Next, a quantitative hazard rating must be established to determine whether the missile should be destroyed now or at some time later, or not at all. Thus, this footprint that has been computed is used to determine a casualty expectation.

4) The system can advise on the basis of pre-established criteria whether the flight should be aborted. If failure does occur and subsequent flight termination or destruct is initiated by the RSO, the monitoring system will be capable of directing rescue equipment or personnel to areas where debris would be most likely to impact.

5) The Range Safety Center is then to initiate necessary rescue or protection activity.

Figure 1 is a sketch of the typical CRT display planned for EROICA. The blocks at the top show the state of the missile, and are green, amber, or red according to the usual convention to denote normal, deficient or abnormal, or failure modes. Typical quantities for display in these top blocks are chamber pressure, engine gimbal angle, staging events, platform angles, and power-supply voltages. This part of the display is analogous to aircraft monitoring systems, where the pilot need not be concerned with various subsystems as long as he has a green board. The middle of the screen indicates where the missile and debris would fall if the RSO were to destroy it at that instant. The decision whether to allow a failed missile to proceed, whether to command fuel cutoff, or to command vehicle destruct depends on the value of hazard to life and property as a function of time. For example, if the missile would impact in a broad ocean area the decision would logically be to let it continue until impact. If the missile would impact on land, the decision would depend on whether the hazard is increasing or decreasing; if the hazard is decreasing, fuel cutoff or destruction should be delayed until hazard is at a minimum. The logic for the destruct decision is displayed at the bottom of the CRT screen, including the casualty expectation value, its first derivative to indicate the trend of hazard with time, a "hazardous condition" light triggered when the hazard exceeds a selected value, and a computer-suggested "destruct" indicator.

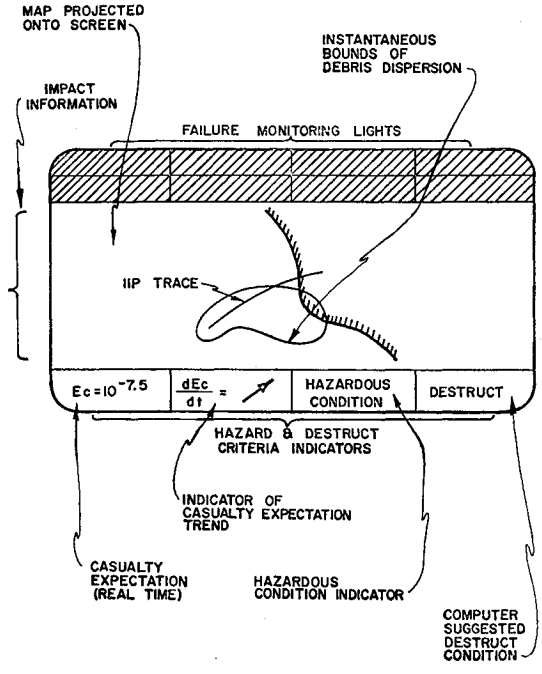

Fig. 1 Typical cathode ray tube display.

EROICA Software Implementation

Within the spectrum of functions performed by a range safety system, those operations that are constrained by real time requirements impose the most serious burdens on the system. They are 1) data acquisition, filtering, and editing, 2) impact prediction, 3) warning computation and hazard prediction, and 4) display generation.

Within the EROICA concept there are two distinct categories of *sensor data*, viz., that data required for impact point prediction and other data. The real-time inputs to the impact predictor are present position and velocity, which are obtained from filtering, smoothing, differentiating, and integrating raw data from sources such as radar and telemetry. Within this raw data, the statistical properties of random errors are usually available, along with information on the correlation of random errors in measurement of distinct variables. Hence a worthwhile effort to remove random errors may be implemented, and there is extensive literature on providing optimum filtering and smoothing under a variety of circumstances.

The *principal hazard* to be determined and displayed under the EROICA system is the expected casualty due to falling debris, assuming a failure and subsequent flight termination. Under the system philosophy which has been developed, the most critical effect of a missile failure is the impact of debris on populated areas; and a primary goal achieved under the concept is the real time display of the most likely impact areas and calculation of both expected casualties and the trend of this expectation. The impact predictors have the property that they are very smooth functions of their input data, i.e., small changes in any parameters such as position, velocity, and so on, produce correspondingly small changes in impact point. This characteristic can be exploited in calculating the areas of most likely debris impact.

The effect of noise errors on impact points can be calculated and expressed as a variance in impact points reached in the downrange and crossrange components. The same is true for errors due to bias uncertainties, thrust termination uncertainties, and wind uncertainties. In addition, there will be a computer lag time which becomes an added uncertainty. Each one of these uncertainties has a known variance, but their effects are trajectory dependent and the distribution of impact points must be computed.

The actual missile breakup results in many pieces of similar ballistic coefficients so that a density of debris particles as a function of ballistic coefficient is a complicated function. Such a function can be approximated by a piecewise linear function if enough data on missile breakup is available. Once

the density function is computed, the expected casualty computation can proceed.

In many current display systems the computer functions as a high-speed data processor to accept data from many sources, correlate and collate as necessary, and present significant data to the operators. In the case of a *display system* for range safety operations, the function of the computer is expanded to include real time computation of the numerous parameters required for manual or automatic decision making. In addition, data relating to missile conditions and instrumentation status requires processing to make it more meaningful. The software for computer generated display systems is a separate programing art. Special programing problems arise wherein tradeoffs between computer hardware and display hardware techniques for utilizing data become factors which must be thoroughly studied in the design of a special system.

EROICA Hardware

The information system developed thus far envisions a comprehensive television screen display which provides the RSO a picture, as complete as possible, of integrated decision data elements in real time. A variety of computers and peripheral devices could be used to implement EROICA. Specific computers will not be discussed, but classes of computers with similar characteristics will be evaluated. The two chief factors which relate to the concept are input/output (I/O) features and central processor organization. The following four classes will be considered: 1) single central processor unit; single channel I/O, non-interlaced; 2) single central processor unit; multiple channel I/O with interlace; 3) multiple central processor units; multiple channel I/O with interlace; and 4) multiple computers with channeling; multiple central processor units in main computer; multiple channel I/O with interlace in main computer. Each class can be configured in three versions: unmodified, modified to include large random access memory units, and modified to a hybrid system with an analog computer.

Greater capacity and program flexibility are obtained with increasing complexity, and this capability is bought for increasing cost. In order to utilize best the distinctive features of each class of computer, however, the system programing must be designed on a speed/accuracy compromise and still achieve the basic goals of the EROICA philosophy. An estimation of the achievability of these goals can be made by measuring the time to execute each of the four crucial tasks, described in the previous section, using programs best designed for each class. The total time is then compared to the time available, and this is set by the system requirements independent of the computer in use. Thus minimal configurations are identified.

Table 1 summarizes system requirements that accomplish the EROICA goals in terms of computer design parameters, for minimum programing. An unmodified Class 1 machine is paced at the fastest throughput rate, which implies instruction execution time of about 200 nanosec per instruction. An unmodified Class 2 machine, by fully utilizing the interruptible, interlaced processor, is paced at approximately the 100-msec rate. This implies execution time of about 600 nanosec per instruction and is again unrealizable.

Unmodified Class 3 and 4 machines with three or more central processor units will satisfy EROICA requirements. Again a Class 4 machine in modified configuration provides exceptional flexibility. In this realm far more accurate models of impact prediction, hazard and casualty, and data filters can be implemented.

Table 1 System requirements

Function	Instruction storage	Inputs	Instructions executed per cycle	Throughput rates
filter	100	radar	100	100 msec
impact prediction	200	4 coefficients	160,000	100 msec
impact prediction	200	8 coefficients	320,000	2 sec
hazard prediction	300	50 population centers 4 fragment categories	1,200	100 msec
display	300	computer data	300	33 msec

Tracking Angle Errors due to Frame Misalignment

ANDREW H. MILSTEAD*
Hughes Aircraft Company, El Segundo, Calif.

TRACKING elevation and/or azimuth errors in the form of residuals or biases that are periodic with respect to azimuth may result from misalignment of the topocentric frame in which elevation and azimuth are measured. This Note presents the derivation of the error formulae resulting from a tilt of the tracking frame about an axis in the horizontal plane. A least-squares procedure is presented by which the misalignment angle, the axis of misalignment and the true bias may be determined from bias or residual data.

Let a topocentric rectangular Cartesian frame be defined with axes directed east (E), north (N), and up (U) as shown in Fig. 1.

Let **e** be the unit vector pointing to a satellite being tracked in the ENU frame. The angles defining the direction of **e** are azimuth (Az) and elevation (El) as shown in Fig. 1. The components of **e** are then given by

$$E = \text{cosEl sinAz} \quad (1)$$

$$N = \text{cosEl cosAz} \quad (2)$$

$$U = \text{sinEl} \quad (3)$$

Suppose now that the ENU frame is rotated by a small angle θ about an axis in the EN (local horizontal) plane which is directed at an angle ϵ measured counter-clockwise from N. Let the rotated frame have axes E', N', and U' (see Fig. 2).

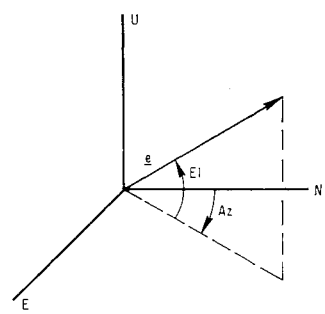

Fig. 1 Topocentric frame.

Received March 6, 1970; revision received May 6, 1970. This work was accomplished while the author was employed at the Aerospace Corporation, El Segundo, Calif.

* Senior Staff Engineer, Space Systems Division. Member AIAA.